JACS
JOURNAL OF THE AMERICAN CHEMICAL SOCIETY

Article

pubs.acs.org/JACS

A Remarkably Complex Supramolecular Hydrogen-Bonded Decameric Capsule Formed from an Enantiopure C_2-Symmetric Monomer by Solvent-Responsive Aggregation

Dovilė Račkauskaitė,[†] Karl-Erik Bergquist,[‡] Qixun Shi,[‡] Anders Sundin,[‡] Eugenijus Butkus,[†] Kenneth Wärnmark,*[,‡] and Edvinas Orentas*[,†]

[†]Department of Organic Chemistry, Vilnius University, Naugarduko 24, LT-03225 Vilnius, Lithuania

[‡]Center for Analysis and Synthesis, Department of Chemistry, Lund University, P.O. Box 124, SE-22100, Lund, Sweden

Supporting Information

ABSTRACT: The formation of an unprecedented decameric capsule in carbon disulfide, held together by the combination of double and triple hydrogen bonds between isocytosine units embedded in an enantiomerically pure bicyclic framework is reported. The aggregation occurs via symmetry breaking of the enantiopure intrinsically C_2-symmetric monomer brought about by solvent, induced tautomerization of the hydrogen-bonding unit. We show that the topology of the aggregate is responsive to the solvent in which the assembly takes place. In this study we demonstrate that in carbon disulfide the chiral decameric cavity aggregate consisting of three forms of the same monomer, differing in their hydrogen bonding to each other is selectively formed, representing a tube-like structure capped with two C_2-symmetric monomers. The large cylindrical cavity produced selectively accommodates one partially solvated C_{60} molecule, and molecular dynamic simulations revealed the special role of the solvent in the inclusion mechanism. The strategy described herein represents the first step toward the creation of a new class of hydrogen-bonded tubular objects from only one small symmetric building block by solvent-responsive aggregation.

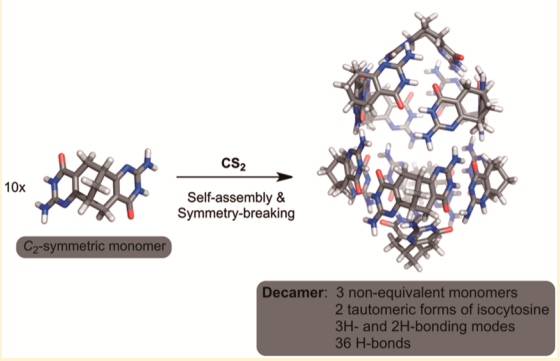

INTRODUCTION

New structures assembled by hydrogen bonding (H-bonding) are of primary importance not only for the advancement of the field of supramolecular chemistry but also for the deeper understanding of the hydrogen-bonding phenomenon in general and the specific role of the solvent in particular.[1] The very useful general guidelines to explain and predict the strength of hydrogen bonds were derived as a result of numerous studies on hydrogen bonding arrays in both solution and the solid state. These include the concept of complementarity and secondary interactions,[2] equilibrium between productive and parasitic tautomeric forms,[3] steric and geometry factors[4] and, acid−base properties of H-bond donors and acceptors.[5] To account for the influence of the media, there is a general agreement that the noncompetitive solvents having neither strong H-bond acceptor nor donor provides the strongest binding. Relatively little, however, is known about more complex systems in which several self-complementary and nonself-complementary tautomeric forms may simultaneously exist within the single monomer capable of producing a cyclic cavity aggregate. In such cases, in addition to the bulk properties of the solvent, the inclusion of it within the cavity formed can no longer be neglected. The solvent molecules acting as small guests can have a decisive role on the selection of the type or the size of the cyclic aggregate.[6] The crucial participation of solvent molecules in the templation of cavity aggregates is very well documented in the field of molecular encapsulation,[7] where the formation of a particular construct is triggered or prevented depending on the size of the solvent molecules.[8]

To achieve tubular aggregation by hydrogen bonding, several conceptual strategies exist that are different from each other in the degree of covalent synthesis used to construct the monomer.[9] In order to secure high predictability of the aggregation process, sophisticated supramolecular monomers having rigid scaffolds with well-defined cavity and H-bonding arrays are often needed.[7,8a−c] The price paid by chemical synthesis to cover the entropic cost of the aggregation process, however, is very high, and often only a single supramolecular construct can be obtained from such monomer as a result of extensive preorganization of the interacting groups. From both a practical and fundamental point of view, it is of paramount importance to find out how far one can go in down-sizing the structure of the monomer and still encode it with as much information as possible in terms of the monomer geometry and nature of the H-bonding array to achieve a specific assembly. Since most of the H-bonding arrays consist of heterocyclic units

Received: March 26, 2015
Published: May 7, 2015

DOI: 10.1021/jacs.5b03160
J. Am. Chem. Soc. 2015, 137, 10536−10546

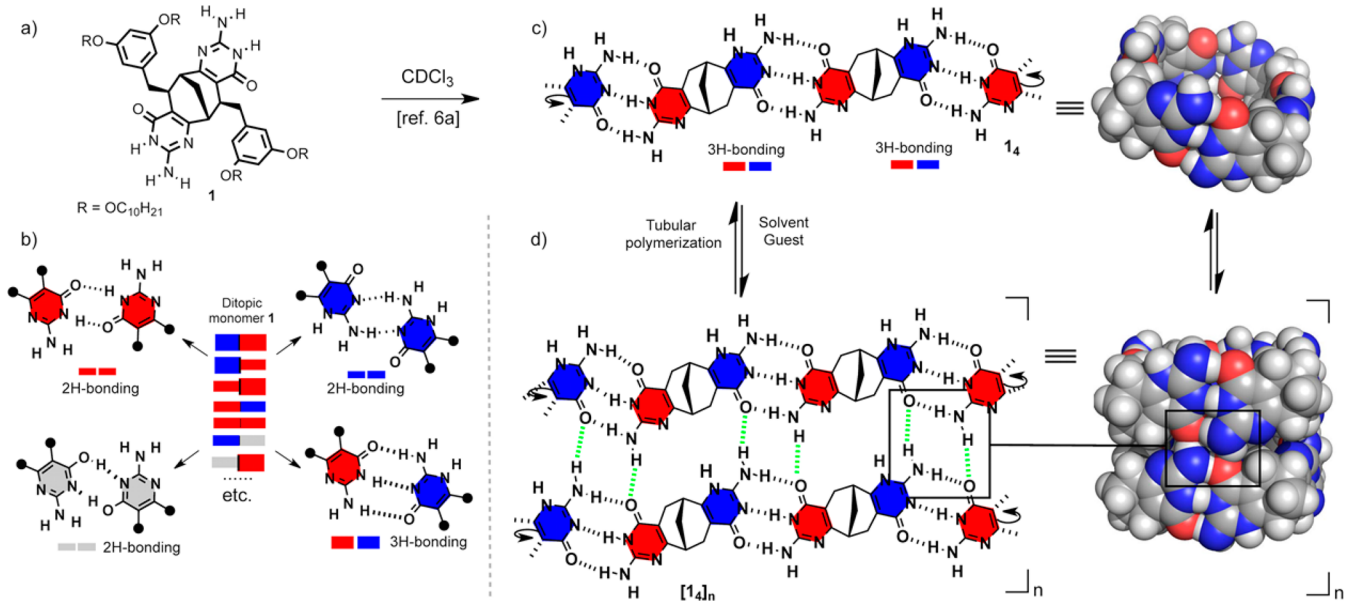

Figure 1. (a) The enantiomerically pure bicyclic ditopic monomer **1** possessing two isocytosine H-bonding moieties. (b) Possible 2H- and 3H-bonding tautomeric forms of the isocytosine (*H*[1], blue; *H*[3], red; and enolic, gray), their distribution in ditopic monomer **1** (several of all conceivable) and the resulting aggregation modes. (c) Formation of a cyclic tetrameric aggregate of **1** in $CDCl_3$ using two complementary tautomeric forms of the isocytosine. (d) The attempted strategy for tubular edge-to-edge polymerization of cyclic tetrameric aggregates $\mathbf{1}_4$ via bifurcated H-bonds (highlighted in square) between cyclic units (solubilizing chains are omitted for clarity).

capable of tautomeric interconversion, the precise control of the aggregation outcome becomes even more complicated. At the same time, the dynamic nature of a H-bonding array might be advantageous for the creation of responsive systems that display multiple aggregation pathways. In such systems, the predominance of one particular tautomeric form will depend on several factors, mainly the polarity of the solvent, the H-bonding mode between the motifs and their spatial arrangement. In this respect, the systems possessing 3H-bonding units are especially interesting due to their intrinsic noncomplementarity owing to the odd number of hydrogen bond donors and acceptors. This apparent drawback can, in principle, be overcome if a certain type of derivatives is used in which tautomerization can bring about self-complementarity between two different tautomeric forms. Among several possibilities, isocytosine derivatives seem to be the perfect candidates to study the relationship between aggregation and tautomeric form distribution. The parent isocytosine is known to crystallize in water in dimeric form held together by 3H-bond between *H*[1] and *H*[3] tautomers (Figure 1b, bottom right).[10,11] We have recently reported that when two isocytosine units are confined within the C_2-symmetric bicyclo[3.3.1]nonane scaffold, the selective formation of a tetrameric cyclic aggregate in chloroform was observed (Figure 1a).[6a] The data obtained suggested that symmetry breaking of the otherwise C_2-symmetric monomer **1** occurred resulting in a 3H-bonded tetramer between the two different tautomeric forms of the isocytosine unit at each end of the molecule. Because of the nearly 90° angle between two H-bonding units, the cyclic tetrameric structure is the most favorable construct; however, our studies on related molecules showed that in certain solvents pentameric assemblies may also form to some extent.[6b] It is worth noting that compound **1** can display many other H-bonding modes depending on the distribution of tautomeric forms within the ditopic monomer. For instance, three different 2H-bonding modes between homoleptic monomers can exist, together with an even larger number of 2H and/or 3H-bonding C_1-symmetric structures (Figure 1b). The cavity size of the cyclic aggregate depends on which particular H-bonding mode is taking place and is therefore the subject of external stimulus modulation, be it solvent or guest. In this article we report our findings from the study of the aggregation of monomer **1** in different solvents. Besides the above-mentioned interest in aggregation induced tautomeric form redistribution, our motivation for this research stemmed from the hypothesis that the cyclic tetramer $\mathbf{1}_4$, a molecular belt, could be forced to aggregate further by using additional complementary bifurcated hydrogen bonding sites along the rim of the tetramer thus producing the desired tubular supramolecular polymers (Figure 1d).[12] Most likely, these intertetramer H-bonds between four isocytosine units (see square in Figure 1d) are significantly weaker than the intratetramer H-bonds assembling the molecular belt $\mathbf{1}_4$ due to the smaller number of hydrogen bonds involved and also due to unfavorable steric interactions between the solubilizing branched side chains when two tetramers approach each other. We therefore speculated that the use of less polar solvents could promote the desired polymerization of $\mathbf{1}_4$ or even change the distribution of tautomeric forms resulting in a new type of assembly. In pursuit of this task we discovered the unexpected formation of a unique decameric aggregate composed of three different forms of the same monomer **1** in the nonpolar solvent carbon disulfide.

RESULTS AND DISCUSSION

Synthesis. Monomer **1** was synthesized according to our previously reported procedure.[6b] ^{13}C and ^{15}N labeled analogues were obtained by using the same methods as for nonlabeled compounds (see the Supporting Information). To secure unambiguous aggregation into cyclic structures, we used the enantiomerically pure monomer **1**, which can be easily obtained in gram quantities from an enzymatically resolved bicyclic precursor.[13] The branched 3,5-bis(decyloxybenzyl) solubilizing

DOI: 10.1021/jacs.5b03160
J. Am. Chem. Soc. 2015, 137, 10536−10546

chains provided very good solubility, which allowed a wide range of nonpolar solvents to be tested in the aggregation studies of **1**.

Self-Assembly of 1 in Different Solvents. The ^{1}H NMR spectra of monomer **1** in different solvents are shown in Figure 2. In contrast to the very well-defined spectral pattern of **1** in $CDCl_3$ (Figure 2a), more complicated spectra were obtained in aromatic solvents. In benzene-d_6 the most intense set of signals is the one belonging to the tetramer $\mathbf{1}_4$, observed together with another set of less intense signals presumably arising from further aggregation of the cyclic aggregates (Figure 2b). In a fresh toluene-d_8 solution, a spectrum containing broad signals was obtained showing a complex pattern of NH resonances of very low intensities. With time, one dominant species evolved; however, the spectrum still showed some minor peaks corresponding to an unknown supramolecular entity (Figure 2c). Interestingly, in a series of chlorinated solvents, the supramolecular tetramer $\mathbf{1}_4$ was the only aggregate observed in relatively polar dichloroethane-d_4 (Figure 2e) as well as in nonpolar carbon tetrachloride (Figure 2d). On the other hand, slightly less polar than chloroform, dichloromethane-d_2 caused the formation of a complex mixture, most likely composed of several aggregates (Figure 2f). We continued to screen different solvents further and found that monomer **1** provided a very clean aggregation profile in the nonpolar solvent carbon disulfide (CS_2) (Figure 2g). CS_2 with the dipole moment p = 0, having a polarizable but poor hydrogen bond acceptor sulfur atom, has rarely been used before for the study of supramolecular aggregates by ^{1}H NMR spectroscopy.[14] Monomer **1**, when dissolved in CS_2, displays a well-defined ^{1}H NMR spectrum possessing 11 different NH resonances together with a complex aromatic and aliphatic pattern (Figure 2g). These features are indicative of a supramolecular structure of significantly reduced symmetry, compared to a chloroform solution of **1**. The formation of a single aggregate was confirmed by the DOSY NMR[15] spectrum that showed a correlation of all resonances with the same diffusion coefficient (see the Supporting Information). Interestingly, when the CS_2 solution of **1** was incrementally diluted with $CDCl_3$, the appearance of the cyclic tetrameric aggregate $\mathbf{1}_4$ was observed at 16% v/v $CDCl_3$ in CS_2 (Figure 3). The two aggregates are in slow equilibrium and the fraction of $\mathbf{1}_4$ is increasing with the addition of $CDCl_3$. The simultaneous existence of two aggregates provided a perfect system for a first estimation of the size of the unknown aggregate by comparing its diffusion coefficient to the one of $\mathbf{1}_4$ under exactly the same experimental conditions. Hence, DOSY measurements of **1** in CS_2–$CDCl_3$ (1:1) indicated that the unknown aggregate is at least 60% larger in hydrodynamic volume than the corresponding cyclic tetramer (see the Supporting Information). These data confirmed that the degree of aggregation of the unknown aggregate is most likely beyond the pentamer for which the increase in the hydrodynamic volume is known to be smaller, based on our earlier studies on urea derivatives of **1**.[16] Finally, it is worth noting that racemic **1** displays completely different aggregation pattern indicating that social self-sorting[17] between

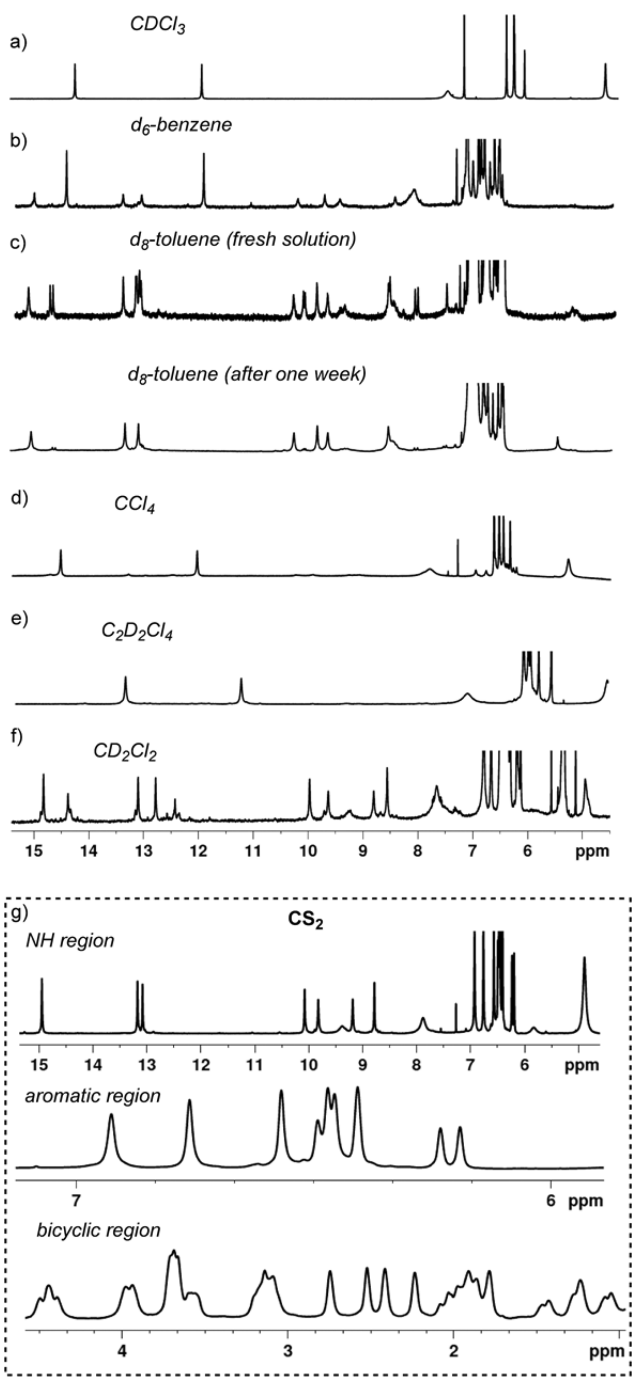

Figure 2. (a–g) Selected parts of ^{1}H NMR spectra of monomer **1** in different solvents.

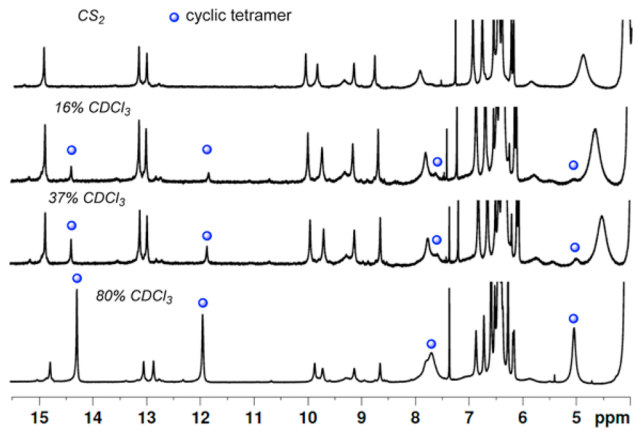

Figure 3. Equilibrium between two different aggregates observed during titration of **1** solution in CS_2 with $CDCl_3$.

DOI: 10.1021/jacs.5b03160
J. Am. Chem. Soc. 2015, 137, 10536–10546

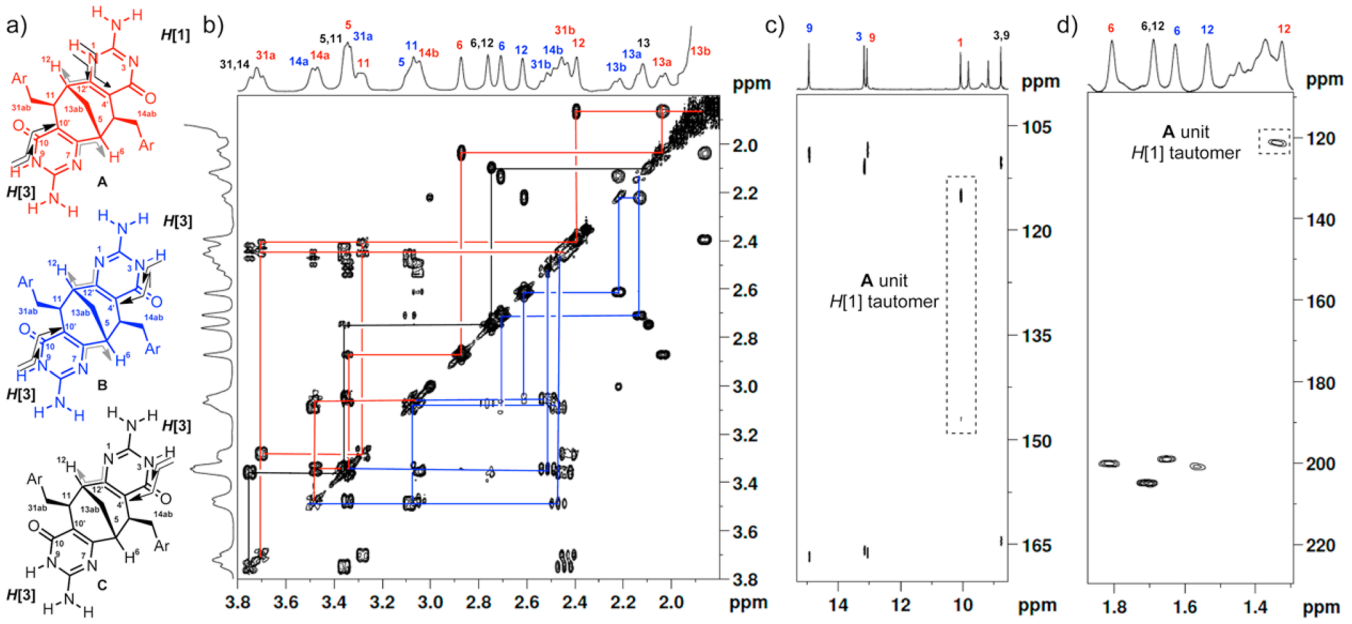

Figure 4. (a) The structures of magnetically nonequivalent units **A**, **B** and **C** observed in the aggregate of **1** in CS_2. The black arrows represent the $^1H-^{13}C$ HMBC correlations and gray arrows the $^1H-^{15}N$ HMBC correlations. (b) COSY spectrum of **1** in CS_2 showing three sets of resonances belonging to units **A**–**C** (color coding as in (a)). (c) $^1H-^{13}C$ HMBC spectrum of **1** in CS_2. (d) $^1H-^{15}N$ HMBC spectrum of **1** in CS_2.

two enantiomers is preferred over homochiral aggregation (see the Supporting Information).

NMR Structure Elucidation of the Aggregate 1_n in CS_2. In order to fully characterize the unknown supramolecular aggregate of **1** in CS_2, extensive NMR studies were undertaken. The careful analysis of the correlations observed in the aliphatic region of the $^1H-^1H$ COSY spectrum of **1** clearly discerned three magnetically nonequivalent monomer units. The units **A** and **B** display sets of resonances corresponding to a C_1-symmetric monomer **1** whereas, in contrast, the third unit **C** must be C_2-symmetric according to the number and pattern of resonances observed (Figure 4a,b). The involvement of the enolic form of the isocytosine moiety in units **A**–**C** was ruled out by the data from the $^1H-^{13}C$ HMBC spectrum, where all the downfield resonances except of proton 1 in **A** and those of the amino groups display couplings with the corresponding carbonyl carbon atoms of the isocytosine keto form. In addition, all the above resonances are from protons residing on nitrogen atoms as shown by the $^1H-^{15}N$ HMQC spectrum. Thus, according to simple symmetry considerations, there is only one intrinsically C_1-symmetric form of **1** where two different keto tautomers of isocytosine, *H*[1] and *H*[3], are located on opposite sides of the monomer. The existence of the *H*[1] tautomeric form in unit **A** is immediately evident from the $^1H-^{13}C$ HMBC spectrum where the NH (1N)-proton resonance at 10.1 ppm shows a diagnostic cross-peak with the carbon atoms of the neighboring double bond at 116 and 146 ppm (Figure 4c), while the ^{13}C NMR gives a chemical shift of 170 ppm for the carbonyl group. The value of the chemical shift of the keto group of the *H*[1] tautomer is in perfect agreement with the recently reported NMR data of hydrogen bonded tautomers of isocytosine in the solid state.[18] Another compelling evidence for the involvement of the *H*[1] tautomer was obtained using the uniformly ^{15}N labeled monomer **1**. The $^1H-^{15}N$ HMBC spectrum revealed that all bridgehead protons 6 and 12 have correlations with the sp^2 nitrogen atoms 1 and 7, respectively, except proton 12 in unit **A**, which has a cross-peak with nitrogen 1 of the *H*[1] tautomer (Figure 4a,d). Accordingly, units **B** and **C** have *H*[3] tautomers on both sides of the bicyclic framework. In contrast to unit **C**, the otherwise identical *H*[3] tautomeric forms in unit **B** become magnetically nonequivalent due to their different environment within the supramolecular aggregate. The existence of the *H*[1] isocytosine tautomer in unit **A** served as a strong indication of the possible involvement of the latter in a 3H-bonding mode. The two distinct aggregation modes, e.g., 2H-bonding between two *H*[3] keto forms and 3H-bonding between *H*[1] and *H*[3] keto forms operating in one C_2-symmetric monomer may be responsible for the symmetry breaking observed in unit **B** (vide infra). The stoichiometry of the assembly was determined from the integration of the ^1H NMR spectrum which gave the molar ratio 2:2:1 for units **A**, **B** and **C**, respectively (see the Supporting Information). This clearly indicated that a pentameric assembly would be the smallest possible candidate whereas based on the DOSY data (vide supra), an even larger structure of the same stoichiometry, i.e., a decamer, is most likely produced.

The next step was to establish the exact connectivity order between the units. We first considered the pentameric cyclic arrangement of previously determined stoichiometry $\mathbf{A_2B_2C}$ as the simplest model (Figure 5a). In a cyclic arrangement, the unit **C** would be connected to unit **A** or **B** via 2H-bonding between *H*[3] tautomeric forms in one of the three possible arrangements, that is **ACA**, **BCB** or **ACB** (Figure 5a, I–III). Consequently, in these models, alternating 2H- and 3H-bonds hold the units **A** and **B** together. If the cyclic pentamer is assumed to be the smallest structural unit, only symmetric **ACA** or **BCB** connectivity is possible in order to maintain the magnetic equivalence of each unit **A** and **B**. To distinguish between these two possible arrangements we used HNN COSY and ROESY experiments. The scalar coupling between two nitrogen atoms across the H-bond constitutes the basis of the HNN COSY experiment and it has been widely utilized in structure elucidation of biomolecules since its introduction.[19]

DOI: 10.1021/jacs.5b03160
J. Am. Chem. Soc. 2015, 137, 10536–10546

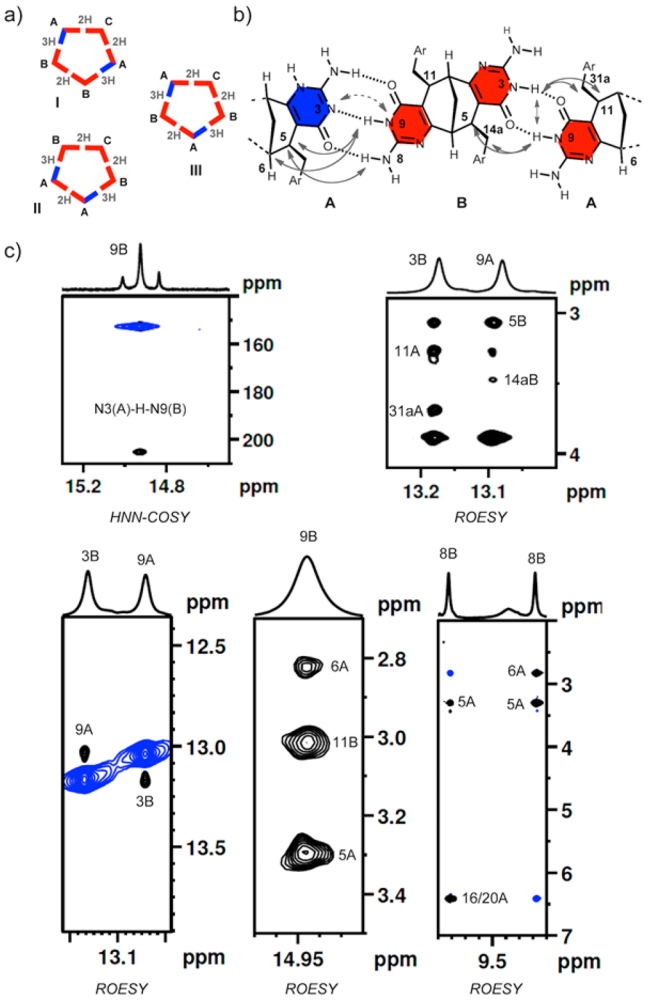

Figure 5. (a) Schematic representation of plausible cyclic pentameric aggregates I–III. (b) Intermolecular NOEs (plain arrows) and scalar N–H–N coupling (dashed arrow) between units **A** and **B**. (c) Excerpts of HNN COSY (top left) and ROESY spectra of **1** in CS_2.

The application of this powerful technique for smaller supramolecular aggregates, however, remains scarce.[20]

The HNN COSY spectrum of uniformly ^{15}N labeled monomer **1** displays scalar coupling between proton 9 of unit **B** and the sp^2 3N atom in the *H*[1] tautomeric site of unit **A** (Figure 5b,c). This observation provided direct evidence that one-half of unit **A** is connected by 3H-bonding to one-half of the unit **B**. Furthermore, the 2H-bonding mode between the *H*[3] tautomeric side of **A** and the other half of **B** was established by the ROESY interaction between proton 9 in **A** and proton 3 in **B** (Figure 5b,c). The proximity of these sites was further supported by the interunit correlation between protons 3 and 9 and the bicyclic and side chain benzylic protons 5,11 and 31,14 of the bonding partner, respectively (Figure 5b). The established monomer sequence corresponds to the cyclic arrangement **ABAB** in which none of the similar NOEs correlations observed between units **A** and **B** could be detected between neither **A** and **C** nor **B** and **C**. Consequently, unit **C** is not a part of the cyclic array. This intriguing fact urged further careful examination of the ROESY spectrum to identify all intermolecular correlations that involve unit **C**. One such correlation was found, namely the NOE between the NH proton in unit **C** and the benzylic proton 11 in unit **B** (Figure 6a). The absence of the ROESY cross-peaks of the aliphatic region of unit **C** with either unit **A** or **B** suggested that this unit is located further away from the **ABAB** tetramer. On the basis of all spectral data, the most plausible arrangement for unit **C** would be on top of the tetramer **ABAB** resulting in pentamer **ABABC**. In this way, the possible network of hydrogen bonds formed between the amino groups in **C** (2N) and carbonyl group in **B**, as well as the amino group in *H*[1] tautomer in **A** (2N) and carbonyl in **C** is in perfect agreement with all spectral data (Figure 6a). On the other hand, some additional correlations between units **A** and **B** clearly indicated that the hitherto suggested pentameric bowl-shaped aggregate was not the final structure of the assembly. In the $^{1}H-^{15}N$ HMBC spectrum there was a coupling between the aromatic nitrogen of the *H*[3] tautomer side of unit **A** and one of the NH protons of 8N amino group in unit **B**. The chemical shifts and the narrow line shape of NH_2 (8N) proton resonances in **B** suggest that both hydrogen atoms are involved in hydrogen bonding and that they are not in fast exchange. Thus, proton 8B, which is a part of the 3H-bonding array is assigned to the chemical shift 9.8 ppm, whereas the other proton at 9.2 ppm is assigned to the hydrogen protruding up and down from the tetramer ring. The HMBC correlation between the hydrogen atom at 9.2 ppm and the nitrogen atom 7 in **A** (Figure 6a) further suggested additional structural complexity beyond the pentameric assembly. This assumption was supported by the ROESY correlation from proton 8B at 9.2 ppm to bridgehead proton 6 in **A** and by the secondary negative NOE from proton 8B at 9.8 ppm to the same proton 6 in **A**. The above correlations cannot be ascribed to neither an **A** nor a **B** unit in the cyclic tetramer simply because these protons are very far away from each other. To account for this observation, the two pentamers have to be connected together by a new H-bonded interface. On the basis of the $^{1}H-^{15}N$ HMBC spectrum, the amino group 8 of unit **B** is hydrogen bonded to the sp^2 nitrogen atom 7 in unit **A**. Likewise the amino group in unit **A** may possibly be hydrogen bonded to the sp^2 nitrogen 7 in unit **B**, although this is neither indicated by NOE nor scalar coupling.[21] In order for these hydrogen bonds to form, two cyclic units have to be turned by 45° in respect to each other.

Now the entire assembly process of the decamer $\mathbf{1}_{10}$ of the composition $[\mathbf{ABABC}]_2$ can be proposed: for clarity, and to illustrate some structural features of the assembly elements the process can be represented in three distinct stages (Figure 6b). First, the alternating tetrameric aggregate **ABAB** is formed using 3H- and 2H-bonding modes of two isocytosine tautomers. The two pairs of opposite walls have 2H- and 3H-bonding interface, which is reflected in the rectangular shape of the tetramer (Figure 6b, stage I). In the 3H-bonding mode, two bicyclic frameworks are brought closer together whereas in the looser 2H-bonding mode the two units are by 1.5 Å further away as indicated by molecular modeling (molecular mechanics). Although at first glance very small, the change in dimensions of the cavity for different H-bonding modes could have crucial consequences for the complexation of certain guests such as C_{60} and C_{70}, where very precise matching of sizes is required for efficient recognition. In the stages II and III, two cyclic tetramers **ABAB** are put on top of each other and the resulting tubular octamer is then capped with two **C** units, respectively, forming an $[\mathbf{ABABC}]_2$ decamer (Figure 6b).

Complexation Study of $\mathbf{1}_{10}$ with C_{60}. In order to take advantage of the large cavity size of the so-suggested decamer, its host–guest chemistry with fullerene C_{60} was probed.[22] According to the size of the cavity, there is, at least in theory,

DOI: 10.1021/jacs.5b03160
J. Am. Chem. Soc. 2015, 137, 10536–10546

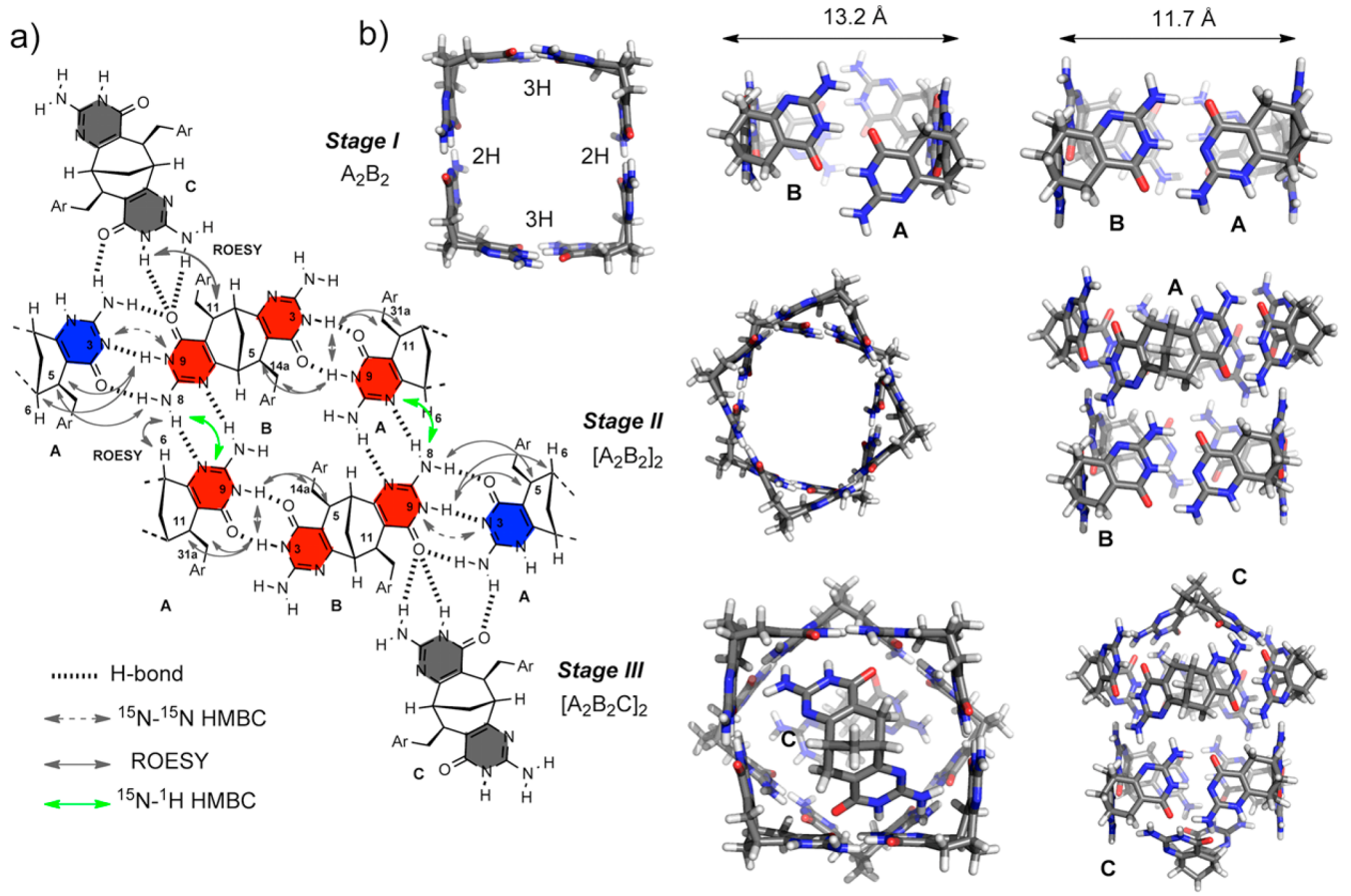

Figure 6. (a) Schematic representation of all interactions observed between units **A**−**C** using different NMR experiments. (b) Simplified illustration of the proposed assembly process in three distinct stages. Stage I, formation of the tetramer; stage II, dimerization of two tetramers; and stage III, capping of the octameric structure with two **C** units. The structures were optimized using molecular mechanics calculations.

the possibility for two C_{60} molecules to be encapsulated if the units **C** are moved further away from the octamer. One may also envision the dissociation of units **C** leaving the uncapped octamer in order to accommodate two molecules of C_{60}. Taking into account that CS_2 is one of the best solvents for C_{60}, we were interested whether one molecule of C_{60} will enter the cavity in a partially solvated form or as two fully desolvated molecules. In the latter process, an additional energetic benefit could be gained from C_{60}−C_{60} van der Waals interaction within the cavity.[22b] Moreover, the host−guest interaction study may also support conclusions drawn from the NMR studies on the structure of the decameric host $\mathbf{1}_{10}$ itself.

Indeed, the decamer $\mathbf{1}_{10}$ formed an inclusion complex with C_{60}; however, full conversion to the host−guest complex was not achieved even with an excess of C_{60} (Figure 7a,b). Two sets of signals were obtained in the ^{1}H NMR spectrum corresponding to the free host and the inclusion complex. The complexation process is accompanied by the large upfield shift of the ^{13}C resonance of C_{60} by 1.0 ppm from 142.7 to 141.7 ppm and also by further reduction of the host symmetry in the C_{60}@$\mathbf{1}_{10}$ complex. The latter is evident from the complication of the aliphatic and aromatic region of the spectrum and the increase of the number of NH resonances. Compared to the free host, each NH resonance is split to two upon the complexation with C_{60} (Figure 7b). The two species displayed identical diffusion coefficients as indicated by the DOSY spectrum confirming that no structural rearrangement to smaller or larger assembly took place during the inclusion event (Figure 7c). The nonsymmetric structure of the complex can be easily rationalized assuming that C_{60} positions itself at one of the poles of the decamer and has a very slow exchange between two identical binding sides that renders the two pentameric hemispheres different (Figure 7a). Since no structural perturbation of the host is taking place during the formation of the inclusion complex, we decided to deploy this equilibrium to unambiguously confirm that the decamer is the actual aggregate in CS_2 solution. The inclusion studies were repeated with ^{13}C labeled monomer **1** and ^{13}C enriched C_{60} guest. By integration of a quantitative ^{13}C spectrum, the stoichiometry was calculated to be exactly 1:10 for the inclusion complex (see the Supporting Information), thus fully corroborating the results obtained from the NMR analysis. Furthermore, these observations show that the host $\mathbf{1}_{10}$ can be a promising candidate also for the encapsulation of larger fullerene guests, such as C_{70}, C_{84} or the dimer C_{120}. To our knowledge, the decameric assembly described here represents the most complicated H-bonded aggregate to date assembled from a small C_2-symmetric building block.[23,24]

Molecular Dynamic (MD) Simulations. Molecular dynamic simulations[25] in CS_2 were employed in order to gain deeper insight into the mechanism of C_{60} encapsulation and the molecular structure of the complex obtained. In all molecular mechanics (MM) calculations, the structure of the monomer **1** was simplified by exchanging the benzylic side chains with methyl groups. The observed $\mathbf{1}_{10}$ aggregate consists of the three

DOI: 10.1021/jacs.5b03160
J. Am. Chem. Soc. 2015, 137, 10536−10546

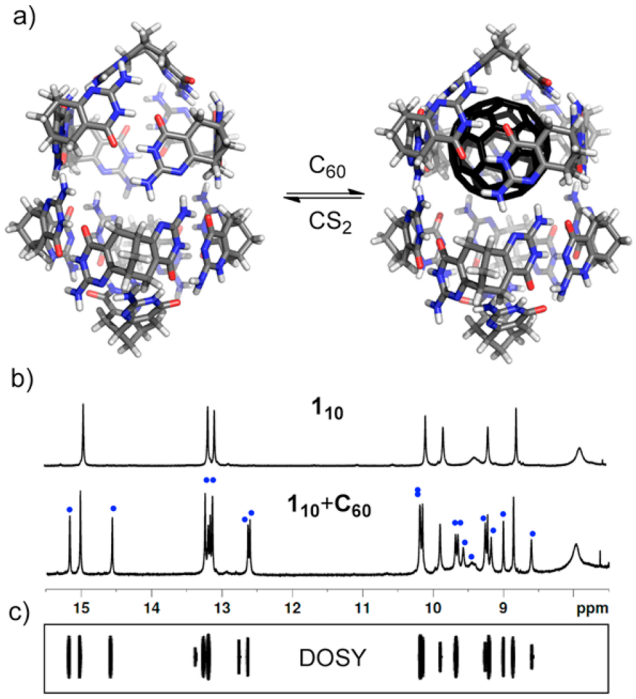

Figure 7. (a) Nonsymmetric complexation of C_{60} with $\mathbf{1}_{10}$ host. (b) ^{1}H NMR spectra of the host $\mathbf{1}_{10}$ (top) and mixture of $\mathbf{1}_{10}$ and inclusion complex $\mathbf{C_{60}@1_{10}}$ (bottom). Saturated solution of C_{60} in CS_2 was used with the molar ratio C_{60}:$\mathbf{1}_{10}$ = 3.7. The blue dots indicate the resonances of $C_{60}@\mathbf{1}_{10}$ (c) DOSY spectrum of the equilibrium mixture of $\mathbf{1}_{10}$ and $C_{60}@\mathbf{1}_{10}$.

forms, **A**, **B** and **C** of monomer **1**, in the proportions 4:4:2 as indicated by the integration of the ^{1}H NMR spectrum.

Models of the final aggregate $\mathbf{1}_{10}$ in CS_2 were constructed in three stages depicted in Figure 6b by applying weak distance constraints for the observed NMR interactions in a geometry optimization using the OPLS 2005 force field in the gas phase. In stage I, a model of the cyclic tetrameric aggregate **ABAB** (Figure 6b) was constructed using the NOE between proton 9 in unit **A** and proton 3 in unit **B** and, between proton 2 in unit **A** and proton 9 in unit **B**. Next, in stage II, an octamer model was assembled by stacking two **ABAB** tetramers (Figure 6b) using the NOE between proton 8 in unit **B** in one tetramer and proton 6 in unit **A** in the other tetramer and the ^{1}H–^{15}N HMBC correlation between proton 8 in unit **B** in one tetramer to nitrogen atom 7 in unit **A** in the other tetramer. A complete model of the decameric aggregate (Figure 6b, Stage III) was constructed from the octamer and two **C** units using constraints based on the NOE correlation between NH_2 in **C** and proton 11 in unit **B**. The resulting decamer $\mathbf{1}_{10}$ is held together by repeated pattern of H-bonds as depicted in Figure 8a.

Molecular dynamics simulations were performed on the gas phase decameric model, extended with a 2,4-ethoxy benzyl side chains as a simplified version of the solubilizing groups. The simulations were performed in the isothermal–isobaric ensemble with a 10 Å buffer of solvent molecules around the complex using Desmond molecular dynamics simulations package with default settings.[26] First, a 9.6 ns MD simulation of the decamer was performed in CS_2. Initially, the simulation had three solvent molecules in the cavity and the system reached equilibrium after 4.5 ns with eight solvent molecules in the cavity (Figure 8b). The inclusion complex with C_{60} was constructed from one snapshot of the equilibrated MD simulation of free $\mathbf{1}_{10}$ in CS_2. All solvent molecules were removed except those in van der Waals contact with the $\mathbf{1}_{10}$ aggregate. A C_{60} molecule was initially positioned at the center of the cavity and all overlapping solvent molecules were removed. Next, a 48 ns MD simulation of this inclusion complex was performed in CS_2. After equilibration, two CS_2 molecules were found situated in the cavity close to one of the **C** units and C_{60} was unsymmetrically placed in the cavity close to the other **C** unit (Figure 8c). The MD simulation thus confirmed that the partial solvation of the C_{60} molecule from one side with CS_2 is responsible for the symmetry breaking of the aggregate. During the equilibration of $\mathbf{1}_{10}$ with C_{60}, the C_{60} molecule moved toward the pole of the capsule, whereas the corresponding interacting unit **C** moved slightly inward as compared to the equilibrium structure of $\mathbf{1}_{10}$ in pure CS_2. The other unit **C** moved slightly outward as a result of an additional

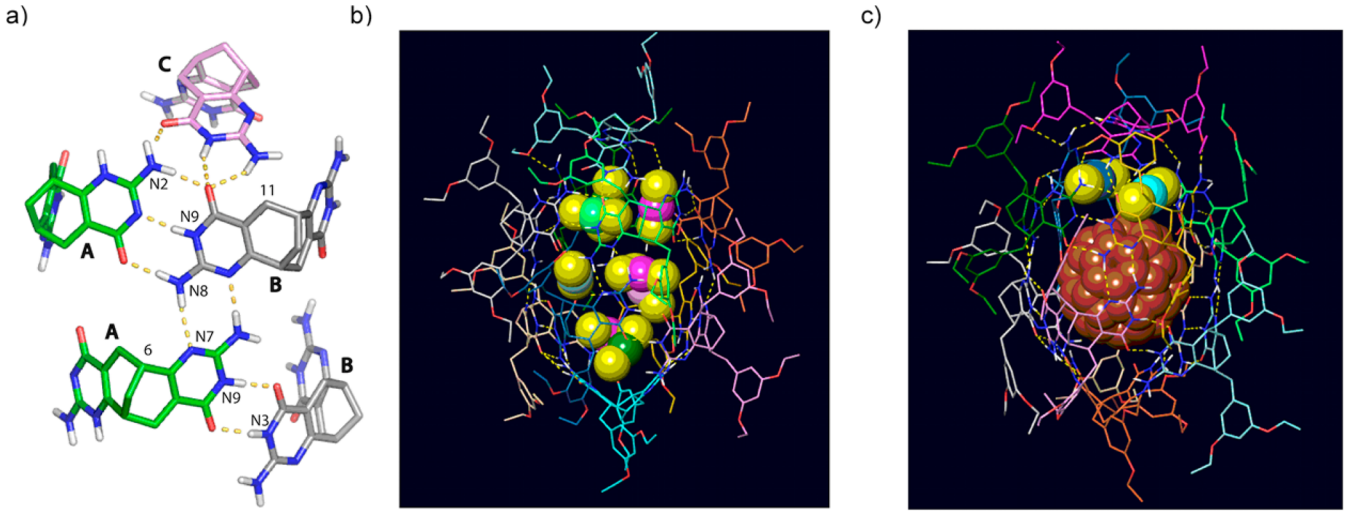

Figure 8. (a) The unique hydrogen bonds of decamer $\mathbf{1}_{10}$ as found by MM calculations. (b) Equilibrated MD structure of $\mathbf{1}_{10}$ in CS_2 with eight solvent molecules in the cavity. (c) Equilibrated MD structure of $C_{60}@\mathbf{1}_{10}$ (t = 46 ns) with two CS_2 molecules. For clarity, solvent molecules outside the cage are not displayed.

DOI: 10.1021/jacs.5b03160
J. Am. Chem. Soc. 2015, 137, 10536–10546

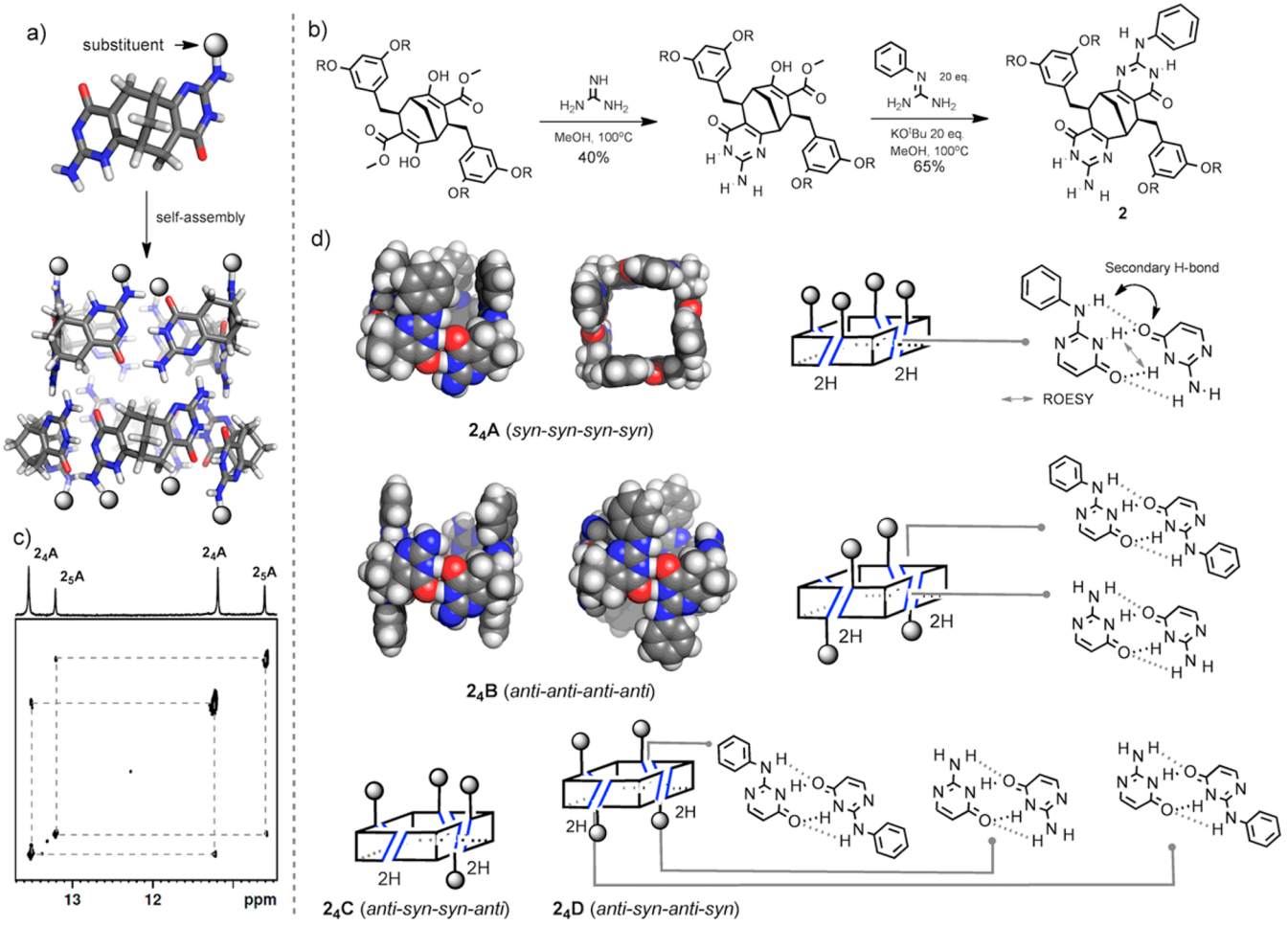

Figure 9. (a) Schematic illustration of monofunctionalization of monomer **1** to selectively produce the octameric aggregate. (b) The synthesis of monomer **2**. (c) The ROESY spectrum of **2** in CS_2. (d) Possible supramolecular isomers of $\mathbf{2}_4$ and the corresponding H-bond interfaces between isocytosine units.

pressure exerted by encapsulated CS_2 molecules. The net reduction in the distance between units **C** was around 0.7 Å. Moreover, the hinge angle between two isocytosine rings was smaller in unit **C** interacting with C_{60} compared to the rest of the units. The above results indicate favorable van der Waals interactions between the C_{60} surface and the concave surface of the unit **C**. Since the movement of the C_{60} molecule inside the cavity is accompanied by its partial desolvation, the above-mentioned interaction between C_{60} and unit **C** is obviously stronger than the interaction between C_{60} and CS_2.[27] The very slow exchange of the C_{60} molecule between two poles can be understood taking into account the fact that the two encapsulated CS_2 molecules that are in close contact to C_{60} have to be simultaneously removed from the cavity in order for C_{60} to exchange the binding sites. Such a process must be kinetically very demanding and is therefore not observed.

Self-Assembly of a C_1-Symmetric 2*N*-Arylated Isocytosine Monomer. The decameric aggregate described has an unprecedented structure with two monomer units residing on top of the tubular octamer. In order to investigate the importance of the capping of the tubular octamer $[\mathbf{ABAB}]_2$ with two **C** units for the stability of the whole assembly, we designed an experiment to slightly mutate the structure of monomer **1** and prevent the H-bonding with the **C** units. By using the C_1-symmetric derivative **2** (Figure 9b), having one phenyl group attached to one isocytosine amino group, the assembly could in principle follow the same pathway through stages I and II resulting in the tubular octamer $[\mathbf{ABAB}]_2$ with all the phenyl groups located at the edges (Figure 6b, 9a). However, stage III would be inhibited in this case, first due to the absence of an extra NH hydrogen atom on unit **A** essential for H-bonding with unit **C** and second, due to the steric hindrance imparted by the phenyl substituents. Compound **2** was synthesized in two steps from the corresponding *β*-ketoester by condensing it with guanidine and then with phenylguanidine (Figure 9b) (see the Supporting Information). The phenyl substituent was chosen for its rigidity and also in order to obtain full regioselectivity in the second condensation step. The electron-withdrawing nature of the phenyl substituent renders the nitrogen atom attached to this group less nucleophilic compared to the remaining nitrogen atoms and therefore only 2*N*-substituted isocytosine **2** is obtained. The new monomer showed two sets of signals of nonequal intensities in CS_2 suggesting the presence of two aggregates. In addition, each aggregate has only two H-bonded NH resonances. This simple pattern with two downfield protons per aggregate observed in each supramolecular species corresponds to a 2H-bonded, fully symmetric cyclic assembly and clearly not to the expected octamer. The latter aggregation mode would by necessity involve one hydrogen atom of the amino group in rim-to-rim H-bonding; such H-bond is absent according to ^{1}H NMR data. If the two aggregated species are

DOI: 10.1021/jacs.5b03160
J. Am. Chem. Soc. 2015, 137, 10536−10546

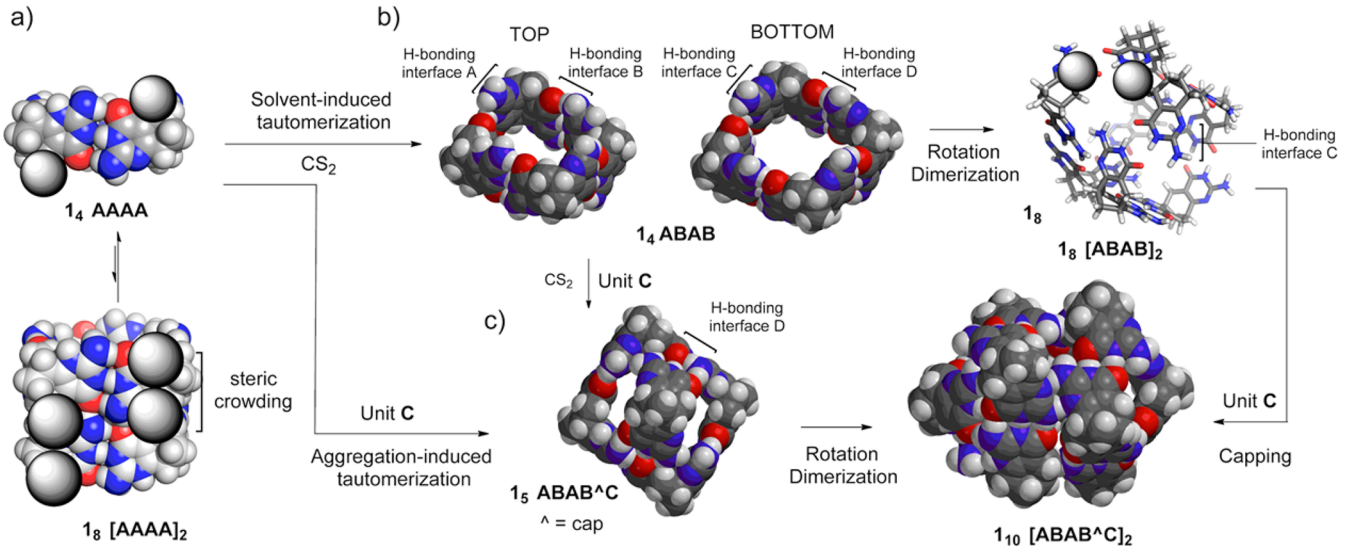

Figure 10. Proposed mechanisms for the formation of decamer $\mathbf{1}_{10}$. (a) Dimerization of the homoleptic tetramer $\mathbf{1}_4$ and the resulting steric repulsion between the bulky substituents. (b) Solvent-induced tautomerization and the subsequent dimerization of so-obtained heteroleptic tetramers. The steric crowding is released to some extent due to the rotation of the tetramers during the dimerization. The decamer $\mathbf{1}_{10}$ is obtained by capping of the octamer. (c) Possible assembly pathways leading to the intermediate pentameric assembly $\mathbf{1}_5$. The decamer $\mathbf{1}_{10}$ is obtained by rotation and dimerization of pentamers $\mathbf{1}_5$ using H-bonding interface A.

assumed to be tetramers, there are in total four possible arrangements for monomer **2**: structure $\mathbf{2}_4\mathbf{A}$ with all phenyl groups on one side (all-*syn* isomer), structure $\mathbf{2}_4\mathbf{B}$ with alternating up and down phenyl groups (all-*anti* isomer) and finally, two less symmetric supramolecular isomers $\mathbf{2}_4\mathbf{C}$ and $\mathbf{2}_4\mathbf{D}$ (Figure 9d). Structures $\mathbf{2}_4\mathbf{C}$ and $\mathbf{2}_4\mathbf{D}$ can immediately be ruled out on the basis of symmetry considerations; only two types of NH signals were observed for each supramolecular isomer. Structures $\mathbf{2}_4\mathbf{A}$ and $\mathbf{2}_4\mathbf{B}$ can be easily distinguished from a ROESY spectrum and the correlation pattern between NH protons. In isomer $\mathbf{2}_4\mathbf{A}$ there must be a cross-peak between two closely located NH protons from two different isocytosine units whereas in isomer $\mathbf{2}_4\mathbf{B}$, both NH protons are identical. Such a correlation was indeed found, unexpectedly for both species, suggesting that in fact only one H-bonding mode is operating and that the two aggregates observed are most likely supramolecular homologues, i.e., a cyclic tetramer and a cyclic pentamer, having the monomer arrangement as in structure $\mathbf{2}_4\mathbf{A}$ with all phenyl groups pointing to the same side (Figure 9c). The final compelling proof was provided by the DOSY spectrum showing the presence of two species of different sizes (see the Supporting Information). The exclusive formation of a supramolecular isomer in which H-bonding occurs only between different isocytosine units could be rationalized by the higher acidity of the phenyl substituted isocytosine NH-group hydrogen bond donor and the higher basicity of the hydrogen bond acceptor carbonyl oxygen on the unsubstituted isocytosine side. There is a possibility that isomer $\mathbf{2}_4\mathbf{A}$ also benefits from a weaker intermolecular secondary hydrogen bond between the phenyl-substituted amino group proton and the carbonyl oxygen. This heteroleptic type of secondary interaction is expected to be stronger than the homoleptic analogues in other possible isomers due to the above-mentioned matching of the acid–base properties of the H-bond donor and acceptor. In contrast to CS_2, only a tetrameric aggregate is formed from the monomer **2** in $CDCl_3$ solution (see the Supporting Information). This observation is in line with the previously observed selectivity in related 4H-bonding derivatives of the monomer **1**, where an exclusive formation of one cyclic tetramers was observed in this solvent.[6b] Although the structural modifications of monomer **1** to compound **2** did not allow to achieve the formation of the octamer in CS_2 by the interrupted $\mathbf{1}_{10}$ self-assembly, the strategy described here provides a new and general method to obtain tetrameric and pentameric cyclic aggregates with a perfect control over the supramolecular isomerism. All attempts to selectively "decapitate" decamer $\mathbf{1}_{10}$ with a 3H-bonding cytosine competitor were met with no success resulting in the disruption of the whole structure (see the Supporting Information).

Analysis of the Assembly Process of 1 in CS_2. Taken together, the above data emphasize the importance of the unsubstituted isocytosine motif for the stabilization of the decameric structure and different tautomeric forms of the ditopic monomer **1** involved in the binding. The intriguing question why the assembly of monomer **1** stops at the decamer stage and does not, for instance, provide polymeric assemblies via repetitive stacking of the tetramers still remains open. If the exact mechanistic details were ignored, entropic factor would favor the formation of a larger number of end-capped decameric assemblies as opposed to a smaller number of polymeric aggregates given the same total number of monomers. The enthalpic gain from weak interoctamer H-bond interactions within the polymer might be too small to outweigh such entropic costs. Another important point of consideration is the interaction of the bulky solubilizing groups within the supramolecular aggregate. The stacking of two homoleptic 3H-bonded tetramers in a fashion originally proposed for the tubular polymerization (Figure 1d) on top of each other without any rotation would place these groups at a short distance resulting in a steric repulsion between two tetramers (Figure 10a).[28] On the other hand, the formation of the octamer held together by 2H- and 3H-bonding modes necessitates the rotation of one of the tetramer and provides the free space to accommodate the solubilizing groups (Figure 10b). The dimerization of the tetramers saturates one of the four H-bonding interfaces present in the tetramer. The

DOI: 10.1021/jacs.5b03160
J. Am. Chem. Soc. 2015, 137, 10536–10546

remaining H-bonding interface D (Figure 10b) in the so-proposed octamer cannot be saturated by the stacking of the octameric aggregates because of the steric interaction between the amino groups along the octamer rims. Instead, the capping with units **C** provides the additional H-bonds resulting in an increase of the total number of H-bonds in the system. Alternatively, the capping of the tetramer **ABAB** with unit **C** may occur before the dimerization event (Figure 10c). We cannot rule out the possibility that the strong H-bonding in CS_2 may promote the attachment of the unit **C** on top of the homoleptic tetramer **AAAA** (Figure 10a) causing the symmetry breaking into alternating 2H- and 3H-bonding modes between isocytosine moieties (aggregation-induced tautomerization), an arrangement that otherwise would be unstable and therefore has not been observed with control compound **2**. The two pentamers **ABABC** obtained would then dimerize minimizing the remaining free H-bond valences. The fact that no octamer was observed with the monophenyl derivative **2** supports the mechanism where capping of the tetramer **ABAB** (or **AAAA**) with unit **C** precedes the dimerization. Regardless of the actual mechanism operating, the crucial role of the solvent is evident. The good polarizability of CS_2, the specific solvation of the cavity or certain tautomeric form of the isocytosine and the promotion of strong hydrogen bonding in this solvent are most likely responsible for very clean and unique aggregation profile of **1**. Having fully deciphered the molecular structure of decamer $\mathbf{1}_{10}$ with the full assignment of all proton resonances, we noticed that very similar pattern of resonances are also seen for **1** in other solvents for the main supramolecular species, especially in dichloromethane-d_2 and in an aged solution in toluene-d_8, indicating the possible formation of the decameric structure in these solvents as well (Figure 2c, 2f). However, only CS_2 afforded very clean, selective and quantitative self-assembly into decameric capsule.

CONCLUSIONS

In conlusion, we have demonstrated for the first time very selective heteroleptic decameric tubular assembly of an enantiopure C_2-symmetric isocytosine derivative in the unconventional solvent carbon disulfide, leading to a decameric capsule unique in the complexity of the H-bonding modes involved. The aggregation process is driven by tautomerization of the isocytosine motif resulting in the simultaneous exploration of both 2H- and 3H-bonding modes. The results presented illustrate the first steps toward the construction of tubular polymers with useful cavity dimensions using small building blocks. Despite the long-lasting extensive research on H-bonded structures, our study demonstrates that this field of supramolecular chemistry is far from being mature. Our study shows that the role of the solvent in the selection of the particular tautomeric form and, hence, the assembly pathway cannot be underestimated. The use of supramolecular monomers capable of tautomeric interconversion is more challenging compared to the static H-bonding arrays; however, it offers new perspectives to achieve highly adaptable systems that provide a large collection of noncovalent topologically different assemblies from the same monomer, depending on the choice of solvent. In addition, this provides economy in the covalent synthesis of the monomer since only *one*, small and C_2-symmetric enantiopure H-bonding block is needed to generate series of diverse supramolecular constructs as a function of the particular solvent used. Such solvent-responsive self-assembly opens new opportunities to the field of adaptive chemistry.[29]

ASSOCIATED CONTENT

Supporting Information

Experimental procedures and spectroscopic data. The Supporting Information is available free of charge on the ACS Publications website at DOI: 10.1021/jacs.5b03160.

AUTHOR INFORMATION

Corresponding Authors

*kenneth.warnmark@chem.lu.se
*edvinas.orentas@chf.vu.lt

Notes

The authors declare no competing financial interest.

ACKNOWLEDGMENTS

The research was funded by European Social Fund under Global Grand Measure (VP1-3.1-ŠMM-07-K-03-007), the Swedish Research Council, the Crafoord Foundation and the Royal Physiographic Society in Lund. Q. S. acknowledges the Wenner-Gren Foundation for a postdoc fellowship. We are grateful to Lukas Taujenis (Department of Analytical and Environmental Chemistry, Vilnius University) for the assistance with mass spectrometry.

REFERENCES

(1) (a) Jeffrey, G. A. *An Introduction to Hydrogen Bonding*; Oxford University Press: New York, 1997. (b) Grabowski, S. J. Hydrogen Bonding—New Insights. In *Series Challenges and Advances in Computational Chemistry and Physics*; Leszczynski, J., Ed.; Springer-Verlag: New York, 2006. (c) Hunter, C. A. *Angew. Chem., Int. Ed.* **2004**, *43*, 5310−5324. (d) Zimmerman, S. C.; Corbin, P. S. *Struct. Bonding (Berlin, Ger.)* **2000**, *96*, 63−94.

(2) (a) Jorgensen, W. L.; Pranata, J. *J. Am. Chem. Soc.* **1990**, *112*, 2008−2010. (b) Pranata, J.; Wierschke, S. G.; Jorgensen, W. L. *J. Am. Chem. Soc.* **1991**, *113*, 2810−2819. (c) Sartorius, J.; Schneider, H.-J. *Chem.—Eur. J.* **1996**, *2*, 1446−1452. (d) Quinn, J. R.; Zimmerman, S. C.; Del Bene, J. E.; Shavitt, I. *J. Am. Chem. Soc.* **2007**, *129*, 934−941.

(3) (a) Beak, P. *Acc. Chem. Res.* **1977**, *10*, 186−192. (b) Beijer, F. H.; Sijbesma, R. P.; Kooijman, H.; Spek, A. L.; Meijer, E. W. *J. Am. Chem. Soc.* **1998**, *120*, 6761−6769. (c) Corbin, P. S.; Zimmerman, S. C. *J. Am. Chem. Soc.* **1998**, *120*, 9710−9711.

(4) (a) Singh, S.; Rao, C. N. R. *J. Am. Chem. Soc.* **1966**, *88*, 2142−2144. (b) Murray, T. J.; Zimmerman, S. C. *Tetrahedron Lett.* **1995**, *36*, 7627−7630.

(5) (a) Kyogoku, Y.; Lord, R. C.; Rich, A. *Proc. Natl. Acad. Sci. U. S. A.* **1967**, *57*, 250−257. (b) Hopkins, H. P.; Alexander, C. J.; Ali, S. Z. *J. Phys. Chem.* **1978**, *82*, 1268−1272.

(6) (a) Orentas, E.; Wallentin, C. J.; Bergquist, K. E.; Lund, M.; Butkus, E.; Wärnmark, K. *Angew. Chem., Int. Ed.* **2011**, *50*, 2071−2074. (b) Shi, Q.; Bergquist, K.-E.; Huo, R.; Li, J.; Lund, M.; Vácha, R.; Sundin, A.; Butkus, E.; Orentas, E.; Wärnmark, K. *J. Am. Chem. Soc.* **2013**, *135*, 15263−15268.

(7) (a) Conn, M. M.; Rebek, J., Jr. *Chem. Rev.* **1997**, *97*, 1647−1668. (b) Rebek, J., Jr. *Angew. Chem., Int. Ed.* **2005**, *44*, 2068−2078. (c) Kobayashi, K.; Yamanaka, M. *Chem. Soc. Rev.* **2015**, *44*, 449−466. (d) Ballester, P. *Isr. J. Chem.* **2011**, *51*, 710−724. (e) Avram, L.; Cohen, Y.; Rebek, J., Jr. *Chem. Commun.* **2011**, *47*, 5368−5375.

(8) (a) Grotzfeld, R. M.; Branda, N.; Rebek, J., Jr. *Science* **1996**, *271*, 487−489. (b) Heinz, T.; Rudkevich, D. M.; Rebek, J., Jr. *Nature* **1998**, *394*, 764−766. (c) Vysotsky, M. O.; Thondorf, I.; Böhmer, V. *Angew. Chem., Int. Ed.* **2000**, *39*, 1264−1267. (d) Avram, L.; Cohen, Y. *J. Am. Chem. Soc.* **2002**, *124*, 15148−15149. (e) Avram, L.; Cohen, Y. *Org. Lett.* **2002**, *4*, 4365−4368. (f) Avram, L.; Cohen, Y. *Org. Lett.* **2003**, *5*, 1099−1102. (g) Avram, L.; Cohen, Y. *Org. Lett.* **2003**, *5*, 3329−3332.

DOI: 10.1021/jacs.5b03160
J. Am. Chem. Soc. 2015, 137, 10536−10546

(h) Avram, L.; Cohen, Y. *Org. Lett.* **2006**, *8*, 219−222. (i) Kvasnica, M.; Chapin, J. C.; Purse, B. W. *Angew. Chem., Int. Ed.* **2011**, *50*, 2244−2248. (j) Shimizu, S.; Kiuchi, T.; Pan, N. *Angew. Chem., Int. Ed.* **2007**, *46*, 6442−6445. (k) Shivanyuk, A.; Friese, J. C.; Döring, S.; Rebek, J., Jr. *J. Org. Chem.* **2003**, *68*, 6489−6496. (l) Shivanyuk, A.; Rebek, J., Jr. *Angew. Chem., Int. Ed.* **2003**, *42*, 684−686. (m) Ajami, D.; Hou, J.-L.; Dale, T. J.; Barrett, E.; Rebek, J., Jr. *Proc. Natl. Acad. Sci. U. S. A.* **2009**, *106*, 10430−10434.

(9) (a) Bong, D. T.; Clark, T. D.; Granja, J. R.; Ghadiri, M. R. *Angew. Chem., Int. Ed.* **2001**, *40*, 988−1011. (b) Balbo Block, M. A.; Kaiser, C.; Khan, A.; Hecht, S. *Top. Curr. Chem.* **2005**, *245*, 89−150.

(10) Connel, J. F.; Sharma, B. D.; Marsh, R. E. *Nature* **1964**, *203*, 399−400.

(11) Abe, H.; Takase, M.; Doi, Y.; Matsumoto, S.; Furusyo, M.; Inouye, M. *Eur. J. Org. Chem.* **2005**, 2931−2940.

(12) For our first approach toward chiral hydrogen-bonded supramolecular polymer, see: Stončius, S.; Orentas, E.; Butkus, E.; Öhrström, L.; Wendt, O. F.; Wärnmark, K. *J. Am. Chem. Soc.* **2006**, *128*, 8272−8285.

(13) Wallentin, C. J.; Orentas, E.; Butkus, E.; Wärnmark, K. *Synthesis* **2009**, *5*, 864−867.

(14) An example of a detailed study of cyclophane host−guest chemistry in different solvents which also included carbon disulfide, see: Smithrud, D. B.; Diederich, F. *J. Am. Chem. Soc.* **1990**, *112*, 339−343.

(15) (a) Branda, T.; Cabritab, E. J.; Berger, S. *Prog. Nucl. Magn. Reson. Spectrosc.* **2005**, *46*, 159−196. (b) Johnson, C. S., Jr. *Prog. Nucl. Magn. Reson. Spectrosc.* **1999**, *34*, 203−256. (c) Cohen, Y.; Avram, L.; Frish, L. *Angew. Chem., Int. Ed.* **2005**, *44*, 520−554. (d) Avram, L.; Cohen, Y. *Chem. Soc. Rev.* **2015**, *44*, 586−602. (e) Evans, R.; Deng, Z.; Rogerson, A. K.; McLachlan, A. S.; Richards, J. J.; Nilsson, M.; Morris, G. A. *Angew. Chem., Int. Ed.* **2013**, *52*, 3199−3202.

(16) The ratio of the diffusion coefficients of cyclic tetramer $\mathbf{1}_4$ and unknown aggregate $\mathbf{1}_n$ was found to be 1.17 in 1:1 (v/v) CS_2-$CDCl_3$ mixture. This value is significantly higher than the one previously found for the mixture of pentamer and tetramer of 4H-bonding urea derivative of **1**. For details, see ref 6b.

(17) (a) Wu, A.; Isaacs, L. *J. Am. Chem. Soc.* **2003**, *125*, 4831−4835. (b) Osowska, K.; Miljanić, O. Š. *Synlett* **2011**, 1643−1648. (c) Safont-Sempere, M. M.; Fernández, G.; Würthner, F. *Chem. Rev.* **2011**, *111*, 5784−5814. (d) Lal Saha, M.; Schmittel, M. *Org. Biomol. Chem.* **2012**, *10*, 4651−4684.

(18) Dračínský, M.; Jansa, P.; Ahonen, K.; Buděšínský, M. *Eur. J. Org. Chem.* **2011**, *8*, 1544−1551.

(19) (a) Dingley, A. J.; Grzesiek, S. *J. Am. Chem. Soc.* **1998**, *120*, 8293−8297. (b) Dingley, A. J.; Cordier, F.; Grzesiek, S. *Concepts Magn. Reson.* **2001**, *13*, 103−127. (c) Dingley, A. J.; Nisius, L.; Cordier, F.; Grzesiek, S. *Nat. Protocols* **2008**, *3*, 242−248.

(20) Söntjens, S. H. M.; van Genderen, M. H. P.; Sijbesma, R. P. *J. Org. Chem.* **2003**, *68*, 9070−9075.

(21) The hydrogen-bonded proton of amino group (8N) in unit **A** would most likely correspond to a nonassigned resonance at 9.41 ppm. Its broadness, however, prevented the correlation with other protons to be observed, whereas the downfield chemical shift indicates its possible involvement in hydrogen bonding.

(22) For H-bonded fullerene receptors, see: (a) Huerta, E.; Metselaar, G. A.; Fragoso, A.; Santos, E.; Bo, C.; de Mendoza, J. *Angew. Chem., Int. Ed.* **2007**, *46*, 202−205. (b) Pantoş, G. D.; Wietor, J. L.; Sanders, J. K. M. *Angew. Chem., Int. Ed.* **2007**, *46*, 2238−2240. (c) Wietor, J.-L.; Pantoş, G. D.; Sanders, J. K. M. *Angew. Chem., Int. Ed.* **2008**, *47*, 2689−2692. (e) Ponnuswamy, N.; Pantos, G. D.; Smulders, M. M. J.; Sanders, J. K. M. *J. Am. Chem. Soc.* **2012**, *134*, 566−573.

(23) (a) Ajami, D.; Rebek, J., Jr. *J. Am. Chem. Soc.* **2006**, *128*, 5314−5315. (b) Tiefenbacher, T.; Ajami, D.; Rebek, J., Jr. *Angew. Chem., Int. Ed.* **2011**, *50*, 12003−12007. (c) Ajami, D.; Rebek, J., Jr. *J. Org. Chem.* **2009**, *74*, 6584−6591. (d) Ghadiri, M. R.; Kobayashi, K.; Granja, J. R.; Chadha, R. K.; McRee, D. E. *Angew. Chem., Int. Ed.* **1995**, *34*, 93−95. (e) Bong, D. T.; Ghadiri, M. R. *Angew. Chem., Int. Ed.* **2001**, *40*, 2163−2166. (f) Amorin, M.; Castedo, L.; Granja, J. R. *J. Am. Chem. Soc.* **2003**, *128*, 2844−2845.

(24) A recent example of unexpectedly complex supramolecular hexamer assembled from simple building block, see: Schaeffer, G.; Fuhr, O.; Fenske, D.; Lehn, J.-M. *Chem.—Eur. J.* **2014**, *20*, 179−186.

(25) *Schrödinger Release 2014−1: Maestro*, version 9.7; Schrödinger, LLC: New York, NY, 2014.

(26) *Schrödinger Release 2014−1: Desmond Molecular Dynamics System*, version 3.7; D. E. Shaw Research: New York, NY, 2014. *Maestro-Desmond Interoperability Tools*, version 3.7; Schrödinger: New York, NY, 2014.

(27) The fact that the complexation of C_{60} with $\mathbf{1}_{10}$ in CS_2 is rather inefficient might be related with the very strong solvation of C_{60} in this solvent. In this case, however, larger number of CS_2 molecules is acting collectively and partially outweighs the interactions between C_{60} and the cavity walls.

(28) Preliminary results in our group indicate that when the bulky substituents are replaced with the linear alkyl chains, the polymerization can indeed be triggered.

(29) Lehn, J.-M. *Chem. Soc. Rev.* **2007**, *35*, 151−160.

DOI: 10.1021/jacs.5b03160
J. Am. Chem. Soc. 2015, 137, 10536−10546